

Kerr effect in quantum dot structure

B. Al-Nashy^{a,c}, S.M.M. Amin^a, Amin H. Al-Khursan^{b,*}

^a College of Science, University of Basrah, Basrah, Iraq

^b Nassiriya Nanotechnology Research Laboratory (NNRL), Science College, Thi-Qar University, Nassiriya, Iraq

^c Science College, Missan University, Missan, Iraq

ARTICLE INFO

Article history:

Received 2 September 2013

Accepted 5 April 2014

ABSTRACT

A three-level ladder QD system is used to study Kerr effect in QD structures. Inhomogenous broadening is included where it is shown to be critical in calculating Kerr effect in QDs. Signal detuning is shown to control Kerr dispersion.

© 2014 Elsevier GmbH. All rights reserved.



1. Introduction

Third order nonlinear real part of susceptibility which known as optical Kerr nonlinearity is of considerable importance due to its applications such as optical communications, quantum optics, quantum computing, optical devices [1,2]. For these applications, the desirable structure must have large nonlinear Kerr with a linear susceptibility as small as possible under low power levels [2]. These requirements are becomes attainable in gases media but not in the solid structures. Accordingly, different solid-state structures are proposed to fit these requirements. For example, electromagnetically induced transparency (EIT) from the four-level systems, spontaneously generated coherence are used in semiconductor structures [3–5]. Although these structures gives a high Kerr nonlinearity compared with linear gain, but it can be enhances many orders of magnitude by the use of nanostructures in the active region which makes it possible for best applications compared with former structures. In these structures, additional levels are crucial to obtain Kerr nonlinearity [5]. Here, a three-level ladder QD system is proposed. A high Kerr nonlinearity is obtained from this structure. This works is organized as follows: Section 2 derives the susceptibility from the equations of motion in the QD structure. Calculations, results and discussion are states in Section 3. Finally, the conclusions from this work are drawn in Section 4.

2. Equations of motion for the QD model

Consider a three-level ladder system, see Fig. 1, with a signal wave deriving the transition from $|1\rangle$ to $|2\rangle$ corresponds to Rabi frequency Ω_s (of frequency w_s) and a probe laser deriving the tran-

sition from $|2\rangle$ and $|3\rangle$ with a Rabi frequency Ω_p (of frequency w_p). Due to the quantum interference between these two absorption baths a spectral transparency window is produced. To obtain nonlinear refractive index, Kerr coefficient began from the dynamical equation of motion for the density matrix which is written as [6],

$$\frac{\partial}{\partial t} \rho_{uv} = -(i\omega_{uv} + \gamma_{uv})\rho_{uv} - \frac{i}{\hbar} [\hat{H}, \hat{\rho}]_{uv} \quad (1)$$

$$H_{uv} = -\frac{1}{2} \mu_{uv} E(\omega) + c.c.,$$

μ_{uv} is the dipole moment. The electric field $E(\omega)$ is expressed as $E(\omega) = E_s e^{-i\omega_s t} + E_p e^{-i\omega_p t}$. To derive the third-order nonlinear Kerr coefficient in a three-level system we must derive $\rho^{(3)}$ which is composed of the two modes s , and p , i.e., $\rho^{(3)} = \sum_{s,p,q} \rho_{s,p,q}^{(3)}$

where

$$\begin{aligned} \rho_{s,p,q}^{(3)} &= \rho_{s,s,p,q}^{(3)}(-\omega_s + \omega_p - \omega_p) + \rho_{s,p,p,q}^{(3)}(-\omega_p + \omega_p - \omega_s) e^{-i\omega_s t} \\ &\quad + \rho_{s,p,q,p}^{(3)}(\omega_p - \omega_p - \omega_s) + \rho_{s,p,q,s}^{(3)}(\omega_p - \omega_s - \omega_p) e^{-i\omega_p t} \end{aligned} \quad (2)$$

Now define,

$$\begin{aligned} \rho_{21}(t) &= \rho_{21} e^{-i\omega_s t}, \\ \rho_{32}(t) &= \rho_{32}(t) e^{-i\omega_p t}, \\ \rho_{31}(t) &= \rho_{31}(t) e^{-i(\omega_s + \omega_p)t}. \end{aligned} \quad (3)$$

This gives for the 1st two terms in Eq. (2),

$$\begin{aligned} &[i(\omega_{21} - \omega_s) + \gamma_{21}] [\rho_{-21}^{(3)}(-\omega_s + \omega_p - \omega_p) + \rho_{-21}^{(3)}(-\omega_p + \omega_p - \omega_s)] e^{-i\omega_s t} \\ &= -\frac{\mu_{21}}{2i\hbar} [\rho_{11}^{(2)}(\omega_s - \omega_p) e^{-i(\omega_s - \omega_p)t} E_p e^{-i\omega_p t} - \rho_{22}^{(2)}(\omega_s - \omega_p) e^{-i(\omega_s - \omega_p)t} E_p e^{-i\omega_p t}] \end{aligned}$$

* Corresponding author.

E-mail address: ameen_2all@yahoo.com (A.H. Al-Khursan).

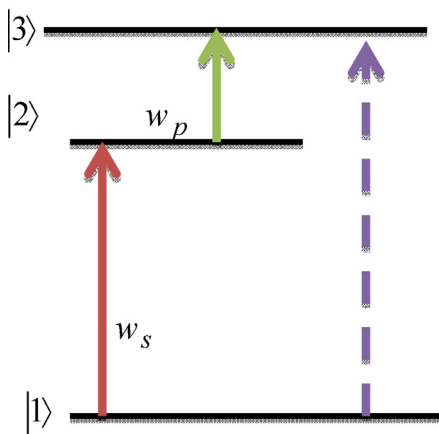


Fig. 1. (a) Schematic of the energy level arrangement under study. The sample with three levels interacts with pump laser (frequency w_s) and a field (frequencies w_p). The dotted line from level $|1\rangle$ to $|3\rangle$ refers to the forbidden transition between them.

$$-\frac{\mu_{21}}{2i\hbar} [\rho_{11}^{(2)}(-\omega_p + \omega_p)e^{-i(\omega_p - \omega_p)t} E_s e^{-i\omega_s t} - \rho_{22}^{(2)}(-\omega_p + \omega_p)e^{-i(\omega_p - \omega_p)t} E_s e^{-i\omega_s t}]. \quad (4)$$

After some mathematical manipulations, one obtains,

$$\begin{aligned} \rho_{21}^{(3)}(s, p, p) = & \frac{|\mu_{21}|^2 E_p^*}{2i\hbar^2} \frac{\Omega_s(\rho_{11}^{(0)} - \rho_{22}^{(0)})E_p}{(\tilde{\gamma}_{21})^2 [1 + (|\Omega_p|^2/\tilde{\gamma}_{31}\tilde{\gamma}_{21})]} \left[\frac{1}{i(\omega_p - \omega_s) + \gamma_{11}} + \frac{1}{\gamma_{11}} \right] \\ & + \frac{\mu_{21}E_p}{2i\hbar^2\tilde{\gamma}_{21}} \left[\frac{\mu_{21}\Omega_s(\rho_{11}^{(0)} - \rho_{22}^{(0)})E_p^*}{\tilde{\gamma}_{21}[1 + (|\Omega_p|^2/\tilde{\gamma}_{31}\tilde{\gamma}_{21})]} \right. \\ & \left. - \left(\frac{\mu_{32}E_s}{\tilde{\gamma}_{23}} \right) \left\{ \Omega_p^*(\rho_{33}^{(0)} - \rho_{22}^{(0)}) - \frac{|\Omega_s|^2\Omega_p^*(\rho_{11}^{(0)} - \rho_{22}^{(0)})}{\tilde{\gamma}_{13}\tilde{\gamma}_{12}[1 - (|\Omega_p|^2/\tilde{\gamma}_{13}\tilde{\gamma}_{12})]} \right\} \right] \times \left[\frac{1}{i(\omega_p - \omega_s) + \gamma_{22}} + \frac{1}{\gamma_{22}} \right] \quad (5) \end{aligned}$$

Note that the signal and pump detunings are defined by $\Delta_s = \omega_{21} - \omega_s$ and $\Delta_p = \omega_{32} - \omega_p$, respectively. The complex detunings are $\tilde{\gamma}_{12}$, $\tilde{\gamma}_{13}$, $\tilde{\gamma}_{23}$, they are defined as $\tilde{\gamma}_{ij} = \gamma_{ij} - i\Delta_m$ for $i, j = 1, 2, 3$ and m represents the corresponding field mode (m or p). $\tilde{\gamma}_{21}$, $\tilde{\gamma}_{31}$ are their complex conjugates. The Rabi frequency is defined as $\Omega = \mu E/2\hbar$. The homogeneous broadening linewidth is assumed to be dephasing dominated and related, through the uncertainty principle, to the dephasing linewidth by [7]

$$\hbar\gamma_H = 2\hbar\gamma = \frac{2\hbar}{T_2}, \quad (6)$$

where T_2 is the dephasing time. Collecting the three terms of $\rho_{21}^{(3)}$, Eq. (2), one obtains the third-order susceptibility in the three-level system, which is written as

$$\begin{aligned} \varepsilon_0\chi^{(3)}(\omega_s) = & \frac{|\mu_{21}|^2\Gamma}{2i\hbar^2V} \frac{|E_p|^2}{1 + \delta_{sp}} \int D(\omega) \left\{ \frac{|\mu_{21}|^2(\rho_{11}^{(0)} - \rho_{22}^{(0)})}{\hbar(\tilde{\gamma}_{21})^2[1 + (|\Omega_p|^2/\tilde{\gamma}_{31}\tilde{\gamma}_{21})]} \left[\frac{1}{i(\omega_p - \omega_s) + \gamma_{11}} + \frac{1}{\gamma_{11}} \right] \right. \\ & + \frac{2}{\tilde{\gamma}_{21}} \left(\frac{|\mu_{21}|^2(\rho_{11}^{(0)} - \rho_{22}^{(0)})}{2\hbar\tilde{\gamma}_{21}[1 + (|\Omega_p|^2/\tilde{\gamma}_{31}\tilde{\gamma}_{21})]} \right) \\ & \left. - \left(\frac{\mu_{32}}{\tilde{\gamma}_{23}} \right) \left[\frac{\mu_{32}^*(\rho_{33}^{(0)} - \rho_{22}^{(0)})}{2\hbar} - \frac{|\Omega_s|^2\mu_{32}^*(\rho_{11}^{(0)} - \rho_{22}^{(0)})}{2\hbar\tilde{\gamma}_{13}\tilde{\gamma}_{12}[1 - (|\Omega_p|^2/\tilde{\gamma}_{13}\tilde{\gamma}_{12})]} \left(\frac{1}{i(\omega_p - \omega_s) + \gamma_{22}} + \frac{1}{\gamma_{22}} \right) \right] \right\} dw \quad (7) \end{aligned}$$

where $D(\omega)$ is the energetic inhomogeneous broadening function, which is given by [8]

$$D(\omega) = \frac{D}{\sqrt{2\pi\sigma^2}} e^{-(\hbar(\omega - \omega_s))^2/2\sigma^2} \quad (8)$$

with D is the total number of states, σ is the spectral width of the Gaussian function, Γ is the optical confinement factor and $\delta_{sp} = 1$ for $s = p$ and $\delta_{sp} = 0$ for $s \neq p$. Note that QD gain is obtained from imaginary part of susceptibility while nonlinear optical Kerr coefficient is obtained from its real part.

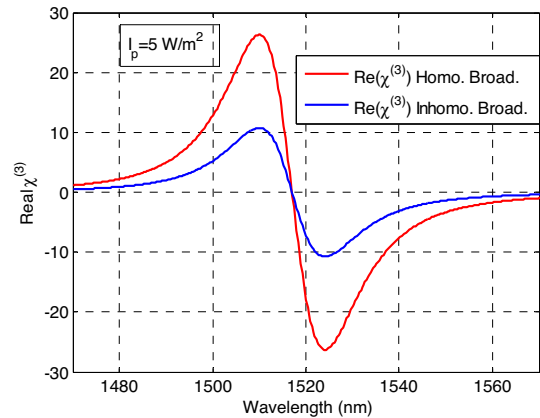


Fig. 2. Real part of nonlinear susceptibility with (blue) and without (red) inhomogeneous broadening. (For interpretation of the references to color in this figure legend, the reader is referred to the web version of the article.)

3. Calculations, results and discussion

The QD structure used in this theoretical study is a tenfold InAs QD layer with $5 \times 10^{10} \text{ cm}^{-2}$ QD density layer which was grown by molecular beam epitaxy at NanoSemiconductor GmbH in Germany

[9,10]. The QDs are in a form of quantum discs with 14 nm height and 4 nm radius. Each QD array is covered with InGaAs WL and 33 nm thick GaAs barrier layer. Each QD active layer is sandwiched between 1.5 μm thick AlGaAs cladding layer. A maximum coupling between the pump beam and the $|3\rangle$ to $|2\rangle$ transition is obtained by choosing the polarization of the pump light parallel to the QD plane [6]. Due to this, the transition between $|1\rangle$ and $|2\rangle$ is forbidden, see Fig. 1. Unless states otherwise, the parameters used in the calculations were stated in Table 1.

Inhomogenous distribution of QDs is assumed and thus a Gaussian function is used to describe QD dispersion in its susceptibility. The effect of inhomogenous distribution in comparison with

homogenous one is shown in Fig. 2. A considerable reduction in the susceptibility is shown due to inhomogenous distribution. For best

Table 1
Structures parameters used in this study [6,7].

Parameter	Description	The value
Γ	Optical confinement factor	0.02
$\gamma_{11}, \gamma_{22}, \gamma_{21}, \gamma_{23}$	Linewidths (meV)	9.36, 3.29, 5.54, 0.33

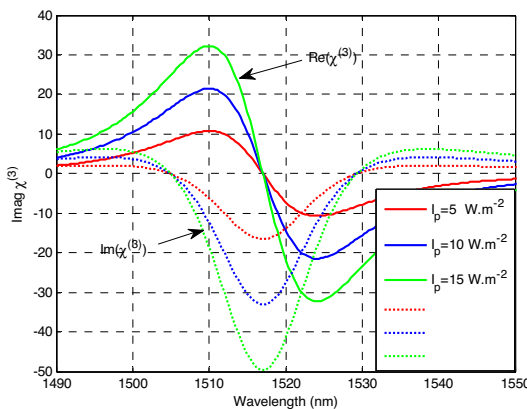


Fig. 3. Nonlinear susceptibility (real and imaginary parts) with inhomogenous broadening at different levels of power density.

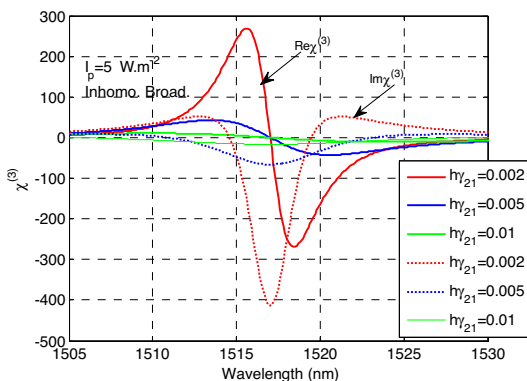


Fig. 4. Nonlinear susceptibility (real and imaginary parts) with inhomogenous broadening at different relaxation energies.

of our knowledge, this is the first work takes QD inhomogeneity into account in the study of Kerr effect. Depending on this result, QD inhomogeneity is critical in the calculation of Kerr effect in QDs. Fig. 3 shows the effect of power level on the real and imaginary parts of nonlinear susceptibility. Different powers are studied (5, 10, and 15 W/m^2). Increasing power level (I_p) increases the Kerr nonlinearity and reduces the absorption. When I_p increases by 5 W/m^2 , the Kerr peak is approximately shifted twice above the absorption peak. Increasing power level is shown not to shifts the frequency peaks of dispersion and absorption.

Fig. 4 shows the effect of relaxation energies $\hbar\gamma_{21}$. Small broadening is shown to give high Kerr dispersion. The peak wavelength is blue shifts with larger broadening. The Kerr dispersion is reduced from 268 (at 1516 nm peak wavelength) to 43 (1514 nm) when the relaxation broadening is increased from 0.002 eV to 0.005 eV. Increasing broadening by order of magnitude (0.01 eV) gives 11 (1510 nm) Kerr dispersion. The Kerr peak is blue shifted with increasing broadening but the transition from anomalous to normal dispersion is still the same. Additionally, shorter linewidth is shown to give high Kerr dispersion. For example, the separation between the peaks of Kerr dispersion and the absorption spectrum at $\hbar\gamma_{21} = 0.002$ eV, is increased by 6 times compared with their separation at $\hbar\gamma_{21} = 0.005$ eV. For shorter linewidth the Kerr peak is red

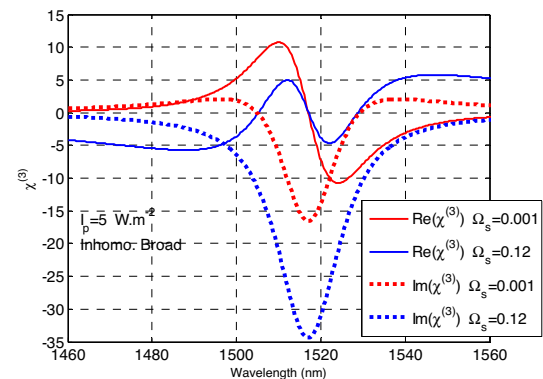


Fig. 5. Real part of nonlinear susceptibility with inhomogenous broadening at different signal detunings.

shifts while the separation between peak Kerr and peak absorption is reduced.

Fig. 5 shows the effect of signal detuning on Kerr dispersion. Signal with very few detuning is shown to give the possibility of slow light. Signal detuning is shown to controls both the peak and strength of Kerr dispersion. This is also seen in double QD structure [11].

4. Conclusions

Using dynamical equation of motion, the third-order nonlinear refractive index (Kerr) dispersion relation is derived. It is shown that inhomogenous broadening is critical in calculating Kerr effect in QDs. Smaller linewidth can reduce the peak absorption and increases Kerr dispersion which can also be controlled by Signal detuning.

References

- [1] H. Kang, Y. Zhu, Observation of large Kerr nonlinearity at low light intensities, *Phys. Rev. Lett.* 91 (2003) 093601.
- [2] J. Kou, R.G. Wan, Z.H. Kang, H.H. Wang, L. Jiang, X.J. Zhang, Y. Jiang, J.Y. Gao, EIT-assisted large cross-Kerr nonlinearity in a four-level inverted-Y atomic system, *J. Opt. Soc. Am. B* 27 (2010) 2035–2039.
- [3] H.R. Hamed, S.H. Asadpour, M. Sahrai, Giant Kerr nonlinearity in a four-level atomic medium, *Optik* 124 (2013) 366–370.
- [4] X. Yan, L. Wang, B. Yin, J. Song, Electromagnetically induced transparency and enhanced self-Kerr nonlinearity in a four-level scheme, *Optik* 122 (2011) 986–990.
- [5] Y. Niu, S. Gong, Enhancing Kerr nonlinearity via spontaneously generated coherence, *Phys. Rev. A* 73 (2006) 053811.
- [6] A.H. Al-Khursan, M.K. Al-Khakani, K.H. Al-Mossawi, Third-order non-linear susceptibility in a three-level QD system, *Photon. Nanostruct. Fundam. Appl.* 7 (2009) 153–160.
- [7] C.J. Chang-Hasnain, P. Ku, J. Kim, S.L. Chuang, Variable optical buffer using slow light in semiconductor nanostructures, *IEEE Proc.* 91 (2003) 1884–1897.
- [8] D. Bimberg, N. Kistaedter, N.N. Ledentsov, Zh. Alferov, P. Kopev, V. Ustinov, In GaAs-GaAs quantum-dot lasers, *IEEE J. Select. Top. Quant. Electron.* 3 (1997) 196–205.
- [9] J. Kim, M. Laemmlin, C. Meuer, D. Bimberg, G. Eisenstein, Static gain saturation model of quantum-dot semiconductor optical amplifiers, *IEEE J. Quantum Electron.* 44 (2008) 658–666.
- [10] S.S. Mikhrin, A.R. Kovsh, I.L. Krestnikov, A.V. Kozhukhov, D.A. Livshits, N.N. Ledentsov, Y.M. Shernyakov, I.I. Novikov, M.V. Maximov, V.M. Ustinov, Z.I. Alferov, High power temperature-insensitive 1.3 μm InAs/InGaAs/GaAs quantum dot lasers, *Semicond. Sci. Technol.* 20 (2005) 340–342.
- [11] X. Hao, J. Wu, Y. Wang, Steady-state absorption-dispersion properties and four wave mixing process in a quantum dot nanostructure; *J. Opt. Soc. Am. B* 29 (2012) 420–428.